HHS Public Access

Author manuscript

Exp Hematol. Author manuscript; available in PMC 2021 February 01.

Published in final edited form as:

Exp Hematol. 2020 February ; 82: 43–52.e4. doi:10.1016/j.exphem.2020.01.014.

Aging-Associated Decrease in the Histone Acetyltransferase KAT6B is Linked to Altered Hematopoietic Stem Cell Differentiation

Eraj Shafiq Khokhar[1,2], **Sneha Borikar**[2], **Elizabeth Eudy**[2], **Tim Stearns**[2], **Kira Young**[2], **Jennifer J. Trowbridge**[1,2,*]

[1]Graduate School of Biomedical Science and Engineering, University of Maine, Orono, ME, 04469

[2]The Jackson Laboratory, Bar Harbor, ME, 04609

Abstract

Aged hematopoietic stem cells (HSCs) undergo biased lineage priming and differentiation toward production of myeloid cells. A comprehensive understanding of gene regulatory mechanisms causing HSC aging is needed to devise new strategies to sustainably improve immune function in aged individuals. Here, a focused shRNA screen of epigenetic factors reveals that the histone acetyltransferase *Kat6b* regulates myeloid cell production from hematopoietic progenitor cells. Within the stem and progenitor cell compartment, *Kat6b* is highly expressed in long-term (LT)-HSCs and is significantly decreased with aging at the transcript and protein levels. Knockdown of *Kat6b* in young LT-HSCs causes skewed production of myeloid cells at the expense of erythroid cells both *in vitro* and *in vivo*. Transcriptome analysis identifies enrichment of aging and macrophage-associated gene signatures alongside reduced expression of self-renewal and multilineage priming signatures. Together, our work identifies KAT6B as a novel epigenetic regulator of hematopoietic differentiation and a target to improve aged immune function.

Keywords

hematopoiesis; hematopoietic stem cells; Aging; histone aceylation

Introduction

Aging involves progressive decline in many cellular systems, including the immune system. Elderly individuals are more susceptible to infections, leading to more frequent and severe illness (Dorshkind and Swain, 2009). With the global population of individuals aged 65 years and older expected to reach 1.6 billion by 2050 (Gasteiger et al., 2016), there is a

*Correspondence should be addressed to: Jennifer J. Trowbridge, Associate Professor, The Jackson Laboratory, 600 Main Street, Bar Harbor, ME 04609, Tel: (207) 288-6183, jennifer.trowbridge@jax.org.

pressing need to develop novel therapeutic strategies to ameliorate aging-associated decline in immune function.

All mature blood and immune cells are derived from HSCs. Changes in HSCs with aging, including increased frequency, enhanced differentiation toward myeloid cells, and reduction in regeneration capacity (Verovskaya et al., 2019), contribute to aging-associated decline in immune function. Molecular features of aged HSCs include decline in mitochondrial function and epigenetic drift. There has been observed to be a global increase in DNA methylation (Beerman et al., 2013; Sun et al., 2014), and altered levels of histone H3 lysine 4 trimethylation (H3K4me3) and lysine 27 trimethylation (H3K27me3) in both aged murine and human HSCs (Adelman et al., 2019; Sun et al., 2014). Moreover, diminished levels and polarity of histone H4 lysine 16 acetylation (H4K16ac) is associated with loss of regenerative capacity and myeloid lineage skewing of old LT-HSCs (Florian et al., 2012). While these studies support involvement of epigenetic regulatory processes in HSC aging, there remains a lack of comprehensive knowledge of the extent to which epigenetic alterations cause aging-associated changes in HSC function. The goal of this study was to identify epigenetic regulators that cause altered differentiation of HSCs in the context of aging. We report a functional screen to uncover novel epigenetic regulators of altered HSC differentiation with aging, identifying the lysine acetyltransferase *Kat6b*.

KAT6B (MORF) belongs to the MYST family of histone acetyltransferases and is responsible for acetylation of the lysine 23 residue of histone H3 (H3K23ac) (Simó-Riudalbas et al., 2015). Other members of the MYST family, KAT6A (MOZ) and KAT8 (MOF), have known functional roles in hematopoiesis. KAT6A, which catalyzes acetylation of lysine 9 (H3K9ac) and lysine 14 (H3K14ac) residues (Huang et al., 2016), is critical for the emergence and maintenance of HSCs (Katsumoto et al., 2006; Perez-Campo et al., 2009; Sheikh et al., 2016). KAT8, which catalyzes acetylation of H4K16ac, is critical for adult but not early fetal hematopoiesis (Valerio et al., 2017). Here, we investigate and demonstrate a novel role for KAT6B in lineage differentiation of phenotypic LT-HSCs.

Materials and Methods

Experimental Animals

Young (2–4 months) and old (20–23 months) female C57BL/6J and B6.SJL-*Ptprc*^{a} *Pepc*^{b}/BoyJ (B6.CD45.1) were obtained from, and aged within, The Jackson Laboratory. All experiments were approved by The Jackson's Laboratory Institutional Animal Care and Use Committee (IACUC).

Lentiviral Supernatant

pLKO.1 shRNA expression plasmids (Sigma; Supplemental Table 4) were modified by cloning in the GFP cassette from pLKO.3G, a gift from Christophe Benoist & Diane Mathis (Addgene) (Primers listed in Supplemental Table 5). shRNA expression plasmids, RC-CMV-Rev1b, HDMHgpm2 (*gag-pol)*, HDM-tat1b, HDM-VSV-G were transfected into HEK-293T cells (ATCC) using CalPhos™ Mammalian Transfection Kit (Takara Bio). Media was

changed after 24hrs and virus was collected after 48hrs. Virus was titered using NIH/3T3 cells (ATCC).

Primary Cell Isolation

Femurs, tibiae, and iliac crests were harvested to isolate hematopoietic cells from the bone marrow (BM). Ficoll-Paque (GE Healthcare) centrifugation was used to isolate BM mononuclear cells (MNCs). MNCs were stained with fluorochrome-conjugated antibodies from BioLegend, eBiosciences or BD Biosciences: c-Kit (clone 2B8), CD48 (clone HM48–1), CD150 (clone TC15–12F12.2), Sca-1 (clone D7), FLT3 (clone A2F10), mature lineage (Lin) marker mix (B220 (clone RA3–6B2), CD11b (clone M1/70), CD4 (clone RM4–5), CD8a (clone 53–67), Ter-119 (clone TER-119), Gr-1 (clone RB6–8C5), CD5 (clone 53–7.3)) and viability stain propidium iodide (PI). Cells were sorted on a FACSAria (BD Biosciences) as follows: LT-HSC (Lin^- Sca^+ $c\text{-}Kit^+$ $Flt3^-$ $CD150^+$ $CD48^-$) and MPP4 cells (Lin^- Sca^+ $c\text{-}Kit^+$ $Flt3^+$ $CD150^-$).

Transduction of LT-HSC and MPP4 Cells

LT-HSCs were resuspended in SFEMII (StemCell Technologies) supplemented with growth factors described previously (Holmfeldt et al., 2016): Stem cell factor (SCF; 10 ng/ml), thrombopoietin (TPO; 20 ng/ml), insulin-like growth factor 2 (IGF2; 20 ng/ml) and fibroblast growth factor (FGF; 10 ng/ml) (BioLegend or StemCell Technologies) along with 5ug/ml polybrene (Sigma) and 1000 MOI lentiviral supernatant. Cells were spun at 2500rpm for 60min then cultured at 37°C and 5% CO_2 for 48hrs. Transduced GFP^+ cells were sorted on a FACSAria (BD Biosciences). MPP4 cells were transduced as above in media containing IMDM plus 10% FBS, interleukin-3 (IL-3, 10 ng/ml), interleukin-6 (IL-6, 10 ug/ml), interleukin-7 (IL-7, 20 ng/ul), SCF (100 ng/ml), leukemia inhibitory factor (LIF, 20 ng/ml) (Peprotech).

Colony Forming Unit (CFU) Assays

For B-lymphoid CFU assays, 100 GFP^+ cells from transduced MPP4 cells were plated in Methocult M3630 (StemCell Technologies) supplemented with FMS-like tyrosine kinase like 3 ligand (FLT3L; 25 ng/ml) and SCF (50 ng/ml) (Peprotech). For myeloid CFU assays, 100 GFP^+ cells from transduced MPP4 cells or 200 GFP^+ cells from transduced LT-HSCs were plated in Methocult GF M3434 (StemCell Technologies) and cultured at 37°C and 5% CO_2. Scoring of colonies was done between days 7 and 10 using a Nikon Eclipse TS100 inverted microscope. CFU cloning efficiency was calculated as the sum of the myeloid and B-lymphoid colonies divided by the sum of the myeloid and B-lymphoid colonies in the NTC group.

Real-Time PCR

Real-time PCR was performed using RT^2 SYBR Green ROX qPCR Mastermix (Qiagen) using the Viaa7 or QuantStudio 7 Flex (Applied Biosystems). Primer sequences are in Supplemental Table 5.

Immunofluorescence Staining of LT-HSCs

Sorted LT-HSCs were seeded on retronectin-coated coverslips in SFEMII supplemented with SCF (10 ng/ml), TPO (20 ng/ul), IGF2 (20 ng/ul), FGF (10 ng/ul) (BioLegend or StemCell Technologies) for 2hrs, then fixed in 4% PFA. Cells were washed with PBS, permeabilized with 0.2% Triton X-100 in PBS for 20mins and blocked with 10% goat serum (ThermoFisher Scientific) for 20mins. Cells were stained with α-KAT6B (NBP1–92036; Novus Biologicals) for 1hr at room temperature. For secondary antibody, cells were stained with α-Rabbit conjugated with Alexa-568 (A-11036; ThermoFisher Scientific) for 1hr. For antibody blocking experiments, control peptides and peptides encoding the immunogen for the KAT6B antibody (GenScript) were incubated overnight at 4 °C with α-KAT6B before staining as above. Coverslips were mounted on slides with Gold Antifade with DAPI. Imaging was performed with Leica SP8 confocal microscope. Z-stack images were summed and quantification of individual fluorescence intensities was performed by Fiji software (Schindelin et al., 2012). Scale bars in images represent 5um.

In Vivo Transplantation

200–350 transduced GFP^+ cells were combined with 5×10^5 MNCs from B6.CD45.1 mice and retro-orbitally injected into recipient B6.CD45.1 mice after 10Gy. Peripheral blood (PB) from recipient mice was analyzed by flow cytometry 1 month after transplant using CD45.1 (clone A201.7 or clone A20), CD45.2 (clone 104), B220 (clone RA3–6B2), CD3e (clone 145–2C11), CD11b (clone M1/70), Ly6g (clone 1A8), Ly6c (clone HK1.4), Ter-119 (clone TER-119), GR1 (clone RB6–8C5), CD4 (clone GK1.5), CD8a (clone 53–6.72) and CD41 (clone MWReg30) (all BioLegend or BD Biosciences). PB was analyzed on a FACSymphony A5 (BD Biosciences) and data was analyzed using FlowJo software (FlowJo, LLC).

RNA-Seq

Transduced GFP^+ LT-HSCs from 3 independent biological replicates were sorted directly into RLT buffer (Qiagen). Total RNA was isolated from cells using the RNeasy Micro kit (Qiagen). Sample quality was assessed using the Nanodrop 2000 spectrophotometer (ThermoFisher Scientific) and the RNA 6000 Pico LabChip assay (Agilent Technologies). Libraries were prepared by the Genome Technologies core facility at The Jackson Laboratory using the Ovation RNA-seq System V2 (NuGEN Technologies) and Hyper Prep Kit (Kapa Biosystems). Libraries were checked for quality and concentration using the D5000 ScreenTape assay (Agilent Technologies) and quantitative PCR (Kapa Biosystems), according to the manufacturers' instructions. Libraries were pooled and sequenced 75 bp single-end on the NextSeq 500 (Illumina) using NextSeq High Output Kit v2.5 reagents. Raw and processed data was deposited in the Gene Expression Omnibus (GEO accession GSE133304).

RNA-Seq Analysis

Trimmed alignment files (with trimmed base quality value < 30, and 70% of read bases surpassing that threshold) were processed using the RSEM (v1.2.12; RNA-Seq by ExpectationMaximization) software (Li and Dewey, 2011) and the Mus Musculus reference

GRCm38. Alignment was completed using Bowtie 2 (v2.2.0) (Langmead and Salzberg, 2012) and processed using SAMtools (v0.1.18) (Li et al., 2009). Fragment length mean was set to 280 and standard deviation to 50. Expected read counts per gene produced by RSEM were rounded to integer values, filtered to include only genes that have at least two samples within a sample group having a cpm > 1.0, and were passed to edgeR (v3.5.3) (Robinson et al., 2010) for differential expression analysis. The negative binomial conditional common likelihood was maximized to estimate a common dispersion value across all genes. Exact tests were used to elucidate statistical differences between the two sample groups of negative-binomially distributed counts producing *p*-values per test. The Benjamini and Hochberg's algorithm was used to control the false discovery rate (FDR). Features with an *FDR*-adjusted *p*-value < 0.05 were declared significantly differentially expressed. Gene set enrichment analysis (GSEA) (Daly et al., 2003; Subramanian et al., 2005) was performed using previously published old LT-HSC RNA-seq data (Sun et al., 2014) and previously defined gene signatures representing HSCs (Chambers et al., 2007), the self-renewal program (Krivtsov et al., 2006), hematopoietic progenitor cell populations (lymphoid (CLP), granulocyte-macrophage (preGM) and erythroid-megakaryocyte (preMegE, preCFU-E, MkP)) (Sanjuan-Pla et al., 2013), and mature hematopoietic cell populations (M1 and M2 macrophages, monocytes, granulocytes, erythrocytes, CD4+ naïve T cells, CD8+ naïve and activated T cells, B cells and NK cells) (Chambers et al., 2007; Engler et al., 2012; Mantovani et al., 2002; Martinez et al., 2006) (Supplemental Table 3).

Statistical Analysis

Sample groups were compared using an unpaired *t* test, Mann-Whitney test, one-way ANOVA and Holm-Sidak's multiple comparisons test, or two-way ANOVA and Dunnett's multiple comparisons test as indicated in figure legends. Prism (GraphPad Software) was utilized for statistical calculations and graphing.

Results

An shRNA screen identifies *Kat6b* as a novel regulator of hematopoietic differentiation

To identify epigenetic regulators with a functional role in hematopoietic stem and progenitor cell differentiation, we conducted an *in vitro* shRNA screen. To derive candidates for this screen, we used gene expression commons (GEXC) (Seita et al., 2012) to define 2,766 differentially expressed genes between granulocyte macrophage progenitors (GMPs; Lin^- Sca^- c-Kit^+ $CD34^+$ $FcgRII/III^+$) and common lymphoid progenitors (CLPs; Lin^- c-Kit^{int} $Flt3^+$ $IL7Ra^+$ $CD27^+$ $Ly6d^-$), which are committed progenitors for the myeloid and lymphoid lineages, respectively (Figure 1A) (Motonari, 2013). Among these 2,766 genes, gene ontology (GO) enrichment analysis of Reactome pathways (Mi et al., 2017; The Gene Ontology Consortium 2019) revealed significant enrichment of chromatin modifying enzymes (Figure 1B). The 40 enriched genes encoding chromatin modifying enzymes were further subset to 30 genes based on overlap with the GO annotation "regulation of gene expression" (GO:0010468) (Supplemental Figure 1A). Lastly, this gene list was filtered to include those with commercially available shRNA constructs with verified knockdown in murine cell lines, resulting in 16 genes (Supplemental Table 1). To begin functional screening, shRNA expression plasmids for six of these 16 genes were obtained. In addition,

shRNA constructs were obtained for eight genes hypothesized to regulate lineage differentiation using a candidate gene approach (Supplemental Table 2). After cloning, we validated reduced target gene expression from each of these shRNA constructs in the murine 3T3 cells (Supplemental Figure 1B).

Our *in vitro* screen (Figure 1C) utilized multipotent progenitor (MPP4) cells rather than purified LT-HSCs as MPP4 cells have both myeloid and lymphoid differentiation potential (Figure 1A) (Pietras et al., 2015) and, in contrast to LT-HSCs, have efficient clonal *in vitro* differentiation capacity giving rise to both myeloid and lymphoid cells (Young et al., 2016). Relative to NTC, we found that knockdown of our positive control, *Crebbp*, resulted in a nearcomplete loss of CFU capacity and the residual colonies that formed were predominantly myeloid (Figure 1D), consistent with the expected phenotype of *Crebbp* loss (Chan et al., 2011).

In two out of the 14 shRNA constructs evaluated, *Rnf40* (ring finger protein 40) and *Kat6b*, we observed a significant increase in the proportion of myeloid relative to B-lymphoid colonies (Figure 1D, Top panel). Of these, only knockdown of *Kat6b* was found not to alter overall cloning efficiency (Figure 1D, Bottom panel) and was pursued as a candidate epigenetic regulator of hematopoietic stem and progenitor cell differentiation.

KAT6B decreases at the transcript and protein level in old LT-HSCs

As the goal of this study was to identify epigenetic regulators that cause altered differentiation of HSCs in the context of aging, we sought to determine whether *Kat6b* is expressed in phenotypic HSCs and whether this expression is altered with aging. We isolated LT-HSCs (Lin^- Sca^+ c-Kit^+ $Flt3^-$ $CD150^+$ $CD48^-$) and MPP4 cells (Lin^- Sca^+ c-Kit^+ $Flt3^+$ $CD150^-$) by FACS from young (2–4 month) and old (20–23 month) mice. By real-time PCR, we observed that the *Kat6b* transcript is expressed in LT-HSCs and that its expression decreases 2.8-fold with age in LT-HSCs but not in MPP4 cells (Figure 2A). This is consistent with previous studies finding a decrease in *Kat6b* expression in aged murine LT-HSCs (Sun et al., 2014) and a decrease in *KAT6B* expression in aged human HSCs (Adelman et al., 2019). To analyze KAT6B at the protein level, we immunostained LT-HSCs from young and old mice with a KAT6B antibody (Figure 2B, Supplemental Figure 2). We observed KAT6B expression in LT-HSCs from old mice is significantly lower than in young mice (Figure 2C). Together, our results show that KAT6B is significantly decreased at both the transcript and protein levels in old LT-HSCs.

Knockdown of *Kat6b* in phenotypic LT-HSCs causes reduced erythropoietic activity *in vitro*

To evaluate the functional consequence of reduced expression of *Kat6b* as observed in old LT-HSCs, we utilized a shRNA knockdown approach. LT-HSCs isolated from young mice were transduced with lentivirus containing NTC or a *Kat6b* shRNA expression plasmid (Figure 3A) and plated into *in vitro* myelo-erythroid differentiation CFU assays. From the resultant colonies, we determined that *Kat6b* transcript was reduced by 4.8-fold (Figure 3B). The total number of colonies was not significantly altered compared to NTC (Figure 3C), however, differences were observed with respect to colony composition. Upon knockdown of *Kat6b*, we observed a significant increase in the number of granulocyte-macrophage

(CFU-GM) colonies, a significant decrease in the number of granulocyte-erythrocyte-macrophage-megakaryocyte (CFU-GEMM) colonies and no change in the number of macrophage-only (CFU-M). (Figure 3D). These phenotypes were replicated using a second, independent hairpin against *Kat6b* (Supplemental Figure 3). Our results demonstrate that knockdown of *Kat6b* results in reduced erythropoietic activity and increased myeloid differentiation from phenotypic LT-HSCs *in vitro*.

Knockdown of *Kat6b* in phenotypic LT-HSCs causes increased myeloid differentiation and reduced erythropoietic activity *in vivo*

To evaluate the functional consequence of reduced levels of *Kat6b* in LT-HSCs *in vivo*, we transduced phenotypic LT-HSCs with *Kat6b* knockdown or NTC and transplanted GFP^+ cells into lethally irradiated B6.CD45.1 recipient mice (Figure 4A). In total, 15 recipient mice were transplanted with NTC-transduced cells and 16 recipient mice were transplanted with *Kat6b* sh1transduced cells. From these, 7/15 (46%) and 8/16 (50%) were found to have multilineage engraftment above a threshold of 0.1% donor-derived PB cells at one month post-transplant. Donor-derived engraftment was not significantly different between NTC and *Kat6b* sh1 (Figure 4B). However, mice transplanted with *Kat6b* knockdown cells had a significant increase in the proportion of donor-derived myeloid cells in the PB as compared to NTC (Figure 4C). In addition, there was a significant decrease in donor-derived erythroid cells in the PB of mice transplanted with *Kat6b* knockdown cells compared to NTC (Figure 4D). A trend toward decreased frequency of donor-derived B and T lymphocytes in *Kat6b* knockdown compared to NTC did not reach statistical significance (Figure 4E, F). Together, these results show that knockdown of *Kat6b* causes reduced erythropoietic activity and increased myeloid differentiation *in vivo* without significantly altering repopulation capacity.

Knockdown of *Kat6b* in LT-HSCs Promotes Expression of Aging- and InflammationAssociated Gene Signatures

To investigate the molecular mechanisms underlying altered differentiation after *Kat6b* knockdown, we transduced LT-HSCs with NTC or *Kat6b* sh1 and performed RNA-seq. Unsupervised clustering separated NTC and *Kat6b* knockdown samples (Figure 5A). 252 significantly differentially expressed genes were identified, out of which 127 genes were upregulated and 125 genes were downregulated in *Kat6b* knockdown compared to NTC (Figure 5B). No other KAT histone lysine acetyltransferases were found to be significantly up- or downregulated after *Kat6b* knockdown (Supplemental Figure 4), supporting minimal off-target effects of our shRNA construct on highly related genes and a lack of compensatory upregulation of other family members in this setting.

To test the hypothesis that *Kat6b* knockdown alters expression of gene programs associated with aging and differentiation of LT-HSCs, we performed gene set enrichment analysis (GSEA) (Subramanian et al., 2005). Comparing our RNA-seq data to a compiled LT-HSC aging gene signature (based on the intersection between published datasets by Sun et al., 2014, Wahlestedt et al., 2013 and Beerman et al., 2013) revealed that genes more highly expressed in young versus old LT-HSCs were significantly enriched in NTC versus *Kat6b* knockdown (Figure 5C). Conversely, genes more highly expressed in old versus young LT-HSCs were enriched in *Kat6b* knockdown versus NTC (Figure 5D).

To further interrogate mechanisms underlying the observed change in differentiation of *Kat6b* knockdown cells, unbiased GO enrichment analysis was utilized. This analysis revealed significant alteration of signatures associated with inflammatory response, cytokine production, and defense response in *Kat6b* knockdown versus NTC cells (Figure 5E). We then compared our dataset to previously defined gene signatures representing HSCs (Chambers et al., 2007), the self-renewal program (Krivtsov et al., 2006), hematopoietic progenitor cell populations (lymphoid (CLP), granulocyte-macrophage (preGM) and erythroid-megakaryocyte (preMegE, preCFU-E, MkP)) (Sanjuan-Pla et al., 2013), and mature hematopoietic cell populations (M1 and M2 macrophages, monocytes, granulocytes, erythrocytes, CD4+ naïve T cells, CD8+ naïve and activated T cells, B cells and NK cells) (Chambers et al., 2007; Engler et al., 2012; Mantovani et al., 2002; Martinez et al., 2006) (Supplemental Table 3). This analysis revealed that *Kat6b* knockdown resulted in a significant enrichment of an M1 macrophage signature while NTC cells were enriched in HSC/self-renewal, preGM, monocyte, CLP, NK and CD8+ naïve T cell signatures (Figure 5F). Together, these data suggest that decreased expression of *Kat6b* in phenotypic LT-HSCs impairs multilineage differentiation, as supported by our *in vitro* and *in vivo* data, and permits a transcriptional program promoting myeloid differentiation that is associated with aging.

Discussion

In this study, by employing a shRNA-mediated screen of epigenetic regulators, we have discovered a novel role for *Kat6b* in the context of LT-HSC differentiation with relevance to aging. We have found that KAT6B decreases in old LT-HSCs at the transcript and protein levels. Knockdown of *Kat6b* resulted in an increase in the proportion of myeloid cells and decrease in the proportion of erythroid cells *in vitro* and *in vivo*. Transcriptome analysis performed immediately after *Kat6b* knockdown in LT-HSCs revealed that knockdown resulted in loss of multilineage priming signatures while gaining an expression signature associated with inflammation and M1 pro-inflammatory macrophages. Interestingly, it has been reported that *Kat6b* expression is reduced in macrophages under LPS stimulation, conditions which result in M1 activation (Shukla et al., 2018). Whether decreased *Kat6b* results in priming towards myeloid, and in particular, macrophage, differentiation or decreased *Kat6b* results in a transcriptional state primed for response to inflammation remains to be tested. Together, our results support that *Kat6b* functions as a regulator of hematopoietic differentiation and that decrease in *Kat6b*, as observed in aging, favors myeloid differentiation at the expense of erythroid differentiation.

Our work builds upon literature demonstrating the importance of the MYST family of acetyltransferases for hematopoietic function. KAT6A, a paralogue of KAT6B (Simpson et al., 2012), is critical for differentiation potential of HSCs (Sheikh et al., 2016). *In vitro, Kat6a*deficient BM has reduced total number of colonies in CFU assays and no difference in colony subtypes (Sheikh et al., 2016), whereas we observed that *Kat6b* knockdown results in no change in total number of colonies and a reduction in erythroid-containing colonies. *In vivo*, conditional knockout of *Kat6a* resulted in impaired competitive repopulation capacity and increased ratio of myeloid to lymphoid differentiation (Sheikh et al., 2016), whereas *Kat6b* knockdown resulted in increased frequency of myeloid cells and decreased frequency

of red blood cells. Thus, we propose that KAT6A and KAT6B may have overlapping but distinct roles in hematopoiesis.

In the context of our experiments, LT-HSCs were cultured under *ex vivo* conditions which have been reported to promote HSC self-renewal (Holmfeldt et al., 2016). However, this requirement for *ex vivo* culture for lentiviral transduction is also a caveat in the interpretation of our results. It is possible that some or all of the LT-HSCs seeded into *ex vivo* culture differentiate to progenitors during the 48h transduction culture period. Thus, the *Kat6b* knockdown phenotype we observe may be manifest in either HSCs or their progenitor progeny. We did not observe any BFU-E-only colonies in our *in vitro* CFU assays, which could be lost due to the effect of our culture conditions on erythroid differentiation potential of LT-HSCs.

We speculate that therapeutically increasing levels of KAT6B in old HSCs may rejuvenate aspects of altered functionality, particularly with respect to lineage-balanced differentiation. A recent report by Adelman et al. demonstrated a reduction in active enhancerassociated chromatin modifications at a *KAT6B*-proximal enhancer region in aged versus young human HSCs (Adelman et al., 2019), suggesting that therapeutic approaches to increase enhancer activity may be a viable strategy to boost *Kat6b* expression in old HSCs. Further studies will be required to test whether restoring expression of *Kat6b* in old HSCs to levels observed in young HSCs is sufficient to restore balanced lineage differentiation.

Supplementary Material

Refer to Web version on PubMed Central for supplementary material.

Acknowledgments

This work was supported by the National Institutes of Diabetes and Digestive and Kidney Diseases (NIDDK) grants R01DK118072 and R56DK112947, the Ellison Medical Foundation New Scholar Award in Aging and pilot funds from The Jackson Laboratory's Nathan Shock Center for Excellence in the Basic Biology of Aging (P30AG038070) (J.J.T.). E.S.K. was supported by Thurgood Marshall Tuition Scholarship from University of Maine. K.Y. received support from T32HD007065, the Pyewacket Fund and the American Society of Hematology (ASH) Scholar Award. We thank Tina Mujica, Jennifer SanMiguel, Olivia Erickson, Tara Murphy and Kaiden Waldron-Francis for technical help, experimental and laboratory support. We thank members of Trowbridge Lab, Christopher Baker, Luanne Peters, Derry Roopenian and Dustin Updike for helpful discussions. We acknowledge Mingyang Lu and Vivek Kohar for computational assistance. We thank Genetic Engineering Technologies, Microscopy, Genome Technologies and Flow Cytometry scientific services at The Jackson Laboratory for their contribution to these studies.

References

Adelman ER, Huang H-T, Roisman A, Olsson A, Colaprico A, Qin T, Lindsley RC, Bejar R, Salomonis N, Grimes HL, Figueroa ME. 2019 Aging Human Hematopoietic Stem Cells Manifest Profound Epigenetic Reprogramming of Enhancers That May Predispose to Leukemia. Cancer Discov CD-18–1474. doi:10.1158/2159-8290.CD-18-1474

Beerman I, Bock C, Garrison BS, Smith ZD, Gu H, Meissner A, Rossi DJ. 2013 Proliferationdependent alterations of the DNA methylation landscape underlie hematopoietic stem cell aging. Cell Stem Cell 12:413–425. doi:10.1016/j.stem.2013.01.017 [PubMed: 23415915]

Chambers SM, Boles NC, Lin K-YK, Tierney MP, Bowman TV., Bradfute SB, Chen AJ, Merchant AA, Sirin O, Weksberg DC, Merchant MG, Fisk CJ, Shaw CA, Goodell MA. 2007 Hematopoietic

Fingerprints: An Expression Database of Stem Cells and Their Progeny. Cell Stem Cell 1:578–591. doi:10.1016/j.stem.2007.10.003 [PubMed: 18371395]

Chan W-I, Hannah RL, Dawson MA, Pridans C, Foster D, Joshi A, Gottgens B, Van Deursen JM, Huntly BJP. 2011 The Transcriptional Coactivator Cbp Regulates Self-Renewal and Differentiation in Adult Hematopoietic Stem Cells. Mol Cell Biol 31:5046–5060. doi:10.1128/mcb.05830-11 [PubMed: 22006020]

Daly MJ, Patterson N, Mesirov JP, Golub TR, Tamayo P, Spiegelman B. 2003 PGC-1αresponsive genes involved in oxidative phosphorylation are coordinately downregulated in human diabetes, Nature Genetics.

Dorshkind K, Swain S. 2009 Age-associated declines in immune system development and function: causes, consequences, and reversal. Curr Opin Immunol 21:404–407. doi:10.1016/j.coi.2009.07.001 [PubMed: 19632102]

Engler JR, Robinson AE, Smirnov I, Hodgson JG, Berger MS. 2012 Increased Microglia/Macrophage Gene Expression in a Subset of Adult and Pediatric Astrocytomas. PLoS One 7:43339. doi:10.1371/journal.pone.0043339

Florian MC, Dörr K, Niebel A, Daria D, Schrezenmeier H, Rojewski M, Filippi MD, Hasenberg A, Gunzer M, Scharffetter-Kochanek K, Zheng Y, Geiger H. 2012 Cdc42 activity regulates hematopoietic stem cell aging and rejuvenation. Cell Stem Cell 10:520–530. doi:10.1016/j.stem.2012.04.007 [PubMed: 22560076]

Gasteiger R, Janiga G, Stucht D, Hennemuth A, Friman O, Speck O, Markl M, Preim B. 2016 An Aging World: 2015, International Population Reports. doi:10.1007/978-3-642-193354_63

Holmfeldt P, Ganuza M, Marathe H, He B, Hall T, Kang G, Moen J, Pardieck J, Saulsberry AC, Cico A, Gaut L, McGoldrick D, Finkelstein D, Tan K, McKinney-Freeman S. 2016 Functional screen identifies regulators of murine hematopoietic stem cell repopulation. J Exp Med 213:433–449. doi:10.1084/jem.20150806 [PubMed: 26880577]

Huang F, Abmayr SM, Workman JL. 2016 Regulation of KAT6 Acetyltransferases and Their Roles in Cell Cycle Progression, Stem Cell Maintenance, and Human Disease. Mol Cell Biol 36:1900–1907. doi:10.1128/mcb.00055-16 [PubMed: 27185879]

Katsumoto T, Aikawa Y, Iwama A, Ueda S, Ichikawa H, Ochiya T, Kitabayashi I. 2006 MOZ is essential for maintenance of hematopoietic stem cells. Genes Dev 20:1321–1330. doi:10.1101/gad.1393106 [PubMed: 16702405]

Krivtsov AV, Twomey D, Feng Z, Stubbs MC, Wang Y, Faber J, Levine JE, Wang J, Hahn WC, Gilliland DG, Golub TR, Armstrong SA. 2006 Transformation from committed progenitor to leukaemia stem cell initiated by MLL-AF9. Nature 442:818–822. doi:10.1038/nature04980 [PubMed: 16862118]

Langmead B, Salzberg SL. 2012 Fast gapped-read alignment with Bowtie 2. Nat Methods 9:357–9. doi:10.1038/nmeth.1923 [PubMed: 22388286]

Li B, Dewey CN. 2011 RSEM: accurate transcript quantification from RNA-Seq data with or without a reference genome. doi:10.1186/1471-2105-12-323

Li H, Handsaker B, Wysoker A, Fennell T, Ruan J, Homer N, Marth G, Abecasis G, Durbin R, Project G, Subgroup DP. 2009 The Sequence Alignment/Map format and SAMtools. Bioinforma Appl NOTE 25:2078–2079. doi:10.1093/bioinformatics/btp352

Mantovani A, Sozzani S, Locati M, Allavena P, Sica A. 2002 Macrophage polarization: tumorassociated macrophages as a paradigm for polarized M2 mononuclear phagocytes, TRENDS in Immunology.

Martinez FO, Gordon S, Locati M, Mantovani A. 2006 Transcriptional profiling of the human monocyte-to-macrophage differentiation and polarization: new molecules and patterns of gene expression. J Immunol 177:7303–11. doi:10.4049/jimmunol.177.10.7303 [PubMed: 17082649]

Mi H, Huang X, Muruganujan A, Tang H, Mills C, Kang D, Thomas PD. 2017 PANTHER version 11: Expanded annotation data from Gene Ontology and Reactome pathways, and data analysis tool enhancements. Nucleic Acids Res 45:D183–D189. doi:10.1093/nar/gkw1138 [PubMed: 27899595]

Motonari K 2013 Lymphoid and myeloid lineage commintment in multipotent hematopoietic progenitors. Immunol Rev 31:128–134. doi:10.1002/ana.22528.Toll-like

Perez-Campo FM, Borrow J, Kouskoff V, Lacaud G. 2009 The histone acetyl transferase activity of monocytic leukemia zinc finger is critical for the proliferation of hematopoietic precursors. Blood 113:4866–4874. doi:10.1182/blood-2008-04-152017 [PubMed: 19264921]

Pietras EM, Reynaud D, Kang Y-A, Carlin D, Calero-Nieto FJ, Leavitt AD, Stuart JM, Göttgens B, Passegué E. 2015 Functionally Distinct Subsets of Lineage-Biased Multipotent Progenitors Control Blood Production in Normal and Regenerative Conditions. Cell Stem Cell 17:35–46. doi:10.1016/j.stem.2015.05.003 [PubMed: 26095048]

Robinson MD, Mccarthy DJ, Smyth GK. 2010 edgeR: a Bioconductor package for differential expression analysis of digital gene expression data. Bioinforma Appl NOTE 26:139–140. doi:10.1093/bioinformatics/btp616

Sanjuan-Pla A, Macaulay IC, Jensen CT, Woll PS, Luis TC, Mead A, Moore S, Carella C, Matsuoka S, Jones TB, Chowdhury O, Stenson L, Lutteropp M, Green JCA, Facchini R, Boukarabila H, Grover A, Gambardella A, Thongjuea S, Carrelha J, Tarrant P, Atkinson D, Clark SA, Nerlov C, Jacobsen SEW. 2013 Platelet-biased stem cells reside at the apex of the haematopoietic stem-cell hierarchy. Nature 502:232–236. doi:10.1038/nature12495 [PubMed: 23934107]

Schindelin J, Arganda-Carreras I, Frise E, Kaynig V, Longair M, Pietzsch T, Preibisch S, Rueden C, Saalfeld S, Schmid B, Tinevez J-Y, White DJ, Hartenstein V, Eliceiri K, Tomancak P, Cardona A. 2012 Fiji: an open-source platform for biological-image analysis. Nat Methods 9:676–82. doi:10.1038/nmeth.2019 [PubMed: 22743772]

Seita J, Sahoo D, Rossi DJ, Bhattacharya D, Serwold T, Inlay MA, Ehrlich LIR, Fathman JW, Dill DL, Weissman IL. 2012 Gene expression commons: An open platform for absolute gene expression profiling. PLoS One 7:e40321. doi:10.1371/journal.pone.0040321 [PubMed: 22815738]

Sheikh BN, Yang Y, Schreuder J, Nilsson SK, Bilardi R, Carotta S, Mcrae HM, Metcalf D, Voss AK, Thomas T. 2016 MOZ (KAT6A) is essential for the maintenance of classically defined adult hematopoietic stem cells. Blood 128:2307–2318. doi:10.1182/blood [PubMed: 27663673]

Simó-Riudalbas L, Pérez-Salvia M, Setien F, Villanueva A, Moutinho C, Martínez-Cardús A, Moran S, Berdasco M, Gomez A, Vidal E, Soler M, Heyn H, Vaquero A, De La Torre C, Barceló-Batllori S, Vidal A, Roz L, Pastorino U, Szakszon K, Borck G, Moura CS, Carneiro F, Zondervan I, Savola S, Iwakawa R, Kohno T, Yokota J, Esteller M. 2015 KAT6B is a tumor suppressor histone H3 lysine 23 acetyltransferase undergoing genomic loss in small cell lung cancer. Cancer Res 75:3936–3944. doi:10.1158/0008-5472.CAN-143702 [PubMed: 26208904]

Simpson MA, Deshpande C, Dafou D, Vissers LELM, Woollard WJ, Holder SE, GillessenKaesbach G, Derks R, White SM, Cohen-Snuijf R, Kant SG, Hoefsloot LH, Reardon W, Brunner HG, Bongers EMHF, Trembath RC. 2012 De Novo Mutations of the Gene Encoding the Histone Acetyltransferase KAT6B Cause Genitopatellar Syndrome. Am J Hum Genet 90:290–294. doi:10.1016/j.ajhg.2011.11.024 [PubMed: 22265017]

Subramanian A, Subramanian A, Tamayo P, Tamayo P, Mootha VK, Mootha VK, Mukherjee S, Mukherjee S, Ebert BL, Ebert BL, Gillette M a, Gillette M a, Paulovich A, Paulovich A, Pomeroy SL, Pomeroy SL, Golub TR, Golub TR, Lander ES, Lander ES, Mesirov JP, Mesirov JP. 2005 Gene set enrichment analysis: a knowledge-based approach for interpreting genome-wide expression profiles., Proceedings of the National Academy of Sciences of the United States of America. doi:10.1073/pnas.0506580102

Sun D, Luo M, Jeong M, Rodriguez B, Xia Z, Hannah R, Wang H, Le T, Faull KF, Chen R, Gu H, Bock C, Meissner A, Göttgens B, Darlington GJ, Li W, Goodell MA. 2014 Epigenomic profiling of young and aged HSCs reveals concerted changes during aging that reinforce self-renewal. Cell Stem Cell 14:673–688. doi:10.1016/j.stem.2014.03.002 [PubMed: 24792119]

The Gene Ontology Consortium,Ashburner M, Ball CA, Blake JA, Botstein D, Butler H, Cherry JM, Davis AP, Dolinski K, Dwight SS, Eppig JT, Harris MA, Hill DP, Issel-tarver L, Kasarskis A, Lewis S, Matese JC, Richardson JE, Rubin GM, Sherlock G. 2000 Gene Ontology: tool for the unification of biology. The Gene Ontology Consortium., Nature Genetics. doi:10.1038/75556.Gene

Valerio DG, Xu H, Eisold ME, Woolthuis CM, Pandita TK, Armstrong SA. 2017 Histone acetyltransferase activity of MOF is required for adult but not early fetal hematopoiesis in mice Key Points. Blood 129:48–59. doi:10.1182/blood-2016-05 [PubMed: 27827827]

Verovskaya EV, Dellorusso PV, Passegué E 2019 Losing Sense of Self and Surroundings: Hematopoietic Stem Cell Aging and Leukemic Transformation. Trends Mol Med. doi:10.1016/j.molmed.2019.04.006

Wahlestedt M, Norddahl GL, Sten G, Ugale A, Frisk M-AM, Mattsson R, Deierborg T, Sigvardsson M, Bryder D. 2013 An epigenetic component of hematopoietic stem cell aging amenable to reprogramming into a young state. Blood 121:4257–4264. doi:10.1182/blood2012-11 [PubMed: 23476050]

Young K, Borikar S, Bell R, Kuffler L, Philip V, Trowbridge JJ. 2016 Progressive alterations in multipotent hematopoietic progenitors underlie lymphoid cell loss in aging. J Exp Med 213:2259–2267. doi:10.1084/jem.20160168 [PubMed: 27811054]

Highlights

- Histone acetyltransferase *Kat6b* highly expressed in hematopoietic stem cells
- KAT6B expression is reduced in hematopoietic stem cells with aging
- Reduced *Kat6b* causes decreased erythropoietic activity and increased myeloid differentiation

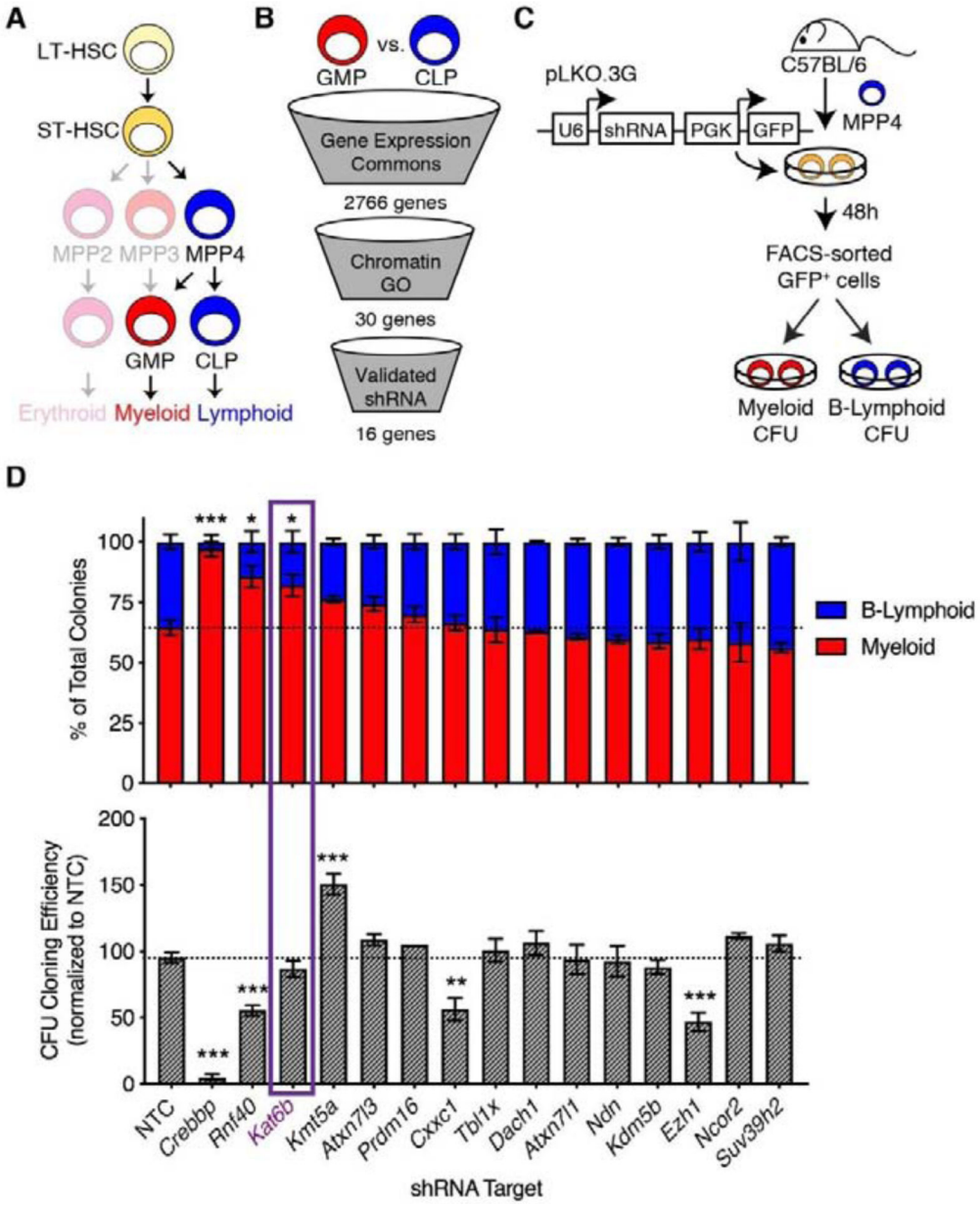

Figure 1. Functional shRNA screen for epigenetic regulators of myeloid versus B-lymphoid differentiation identifies *Kat6b*.

(A) Hierarchy of hematopoietic differentiation showing cellular states leading to mature myeloid and lymphoid cells. (B) Schematic of candidate selection criteria to identify chromatin regulatory genes involved in myeloid versus B-lymphoid differentiation of hematopoietic stem and progenitor cells. GMP; granulocyte-macrophage progenitors, CLP; common lymphoid progenitors. (C) Schematic of experimental design to test epigenetic regulatory gene candidates using shRNA-mediated knockdown in lymphoid-primed multipotent progenitor cells (MPP4) and colony-forming unit (CFU) assays. (D) (Top panel) Frequency of myeloid and B-lymphoid colonies out of total colonies and (Bottom panel) CFU cloning efficiency calculated as the total number of myeloid and B-lymphoid colonies following shRNA knockdown of the indicated target genes divided by the total number of

myeloid and B-lymphoid colonies in NTC. NTC; non-targeting control. Bars represent mean ± SEM of $n \geq 2$ biological replicates. *$P < 0.05$; **$P < 0.01$; ***$P < 0.001$ by two-way ANOVA and Dunnett's multiple comparisons test or one-way ANOVA and Holm-Sidak's multiple comparisons test.

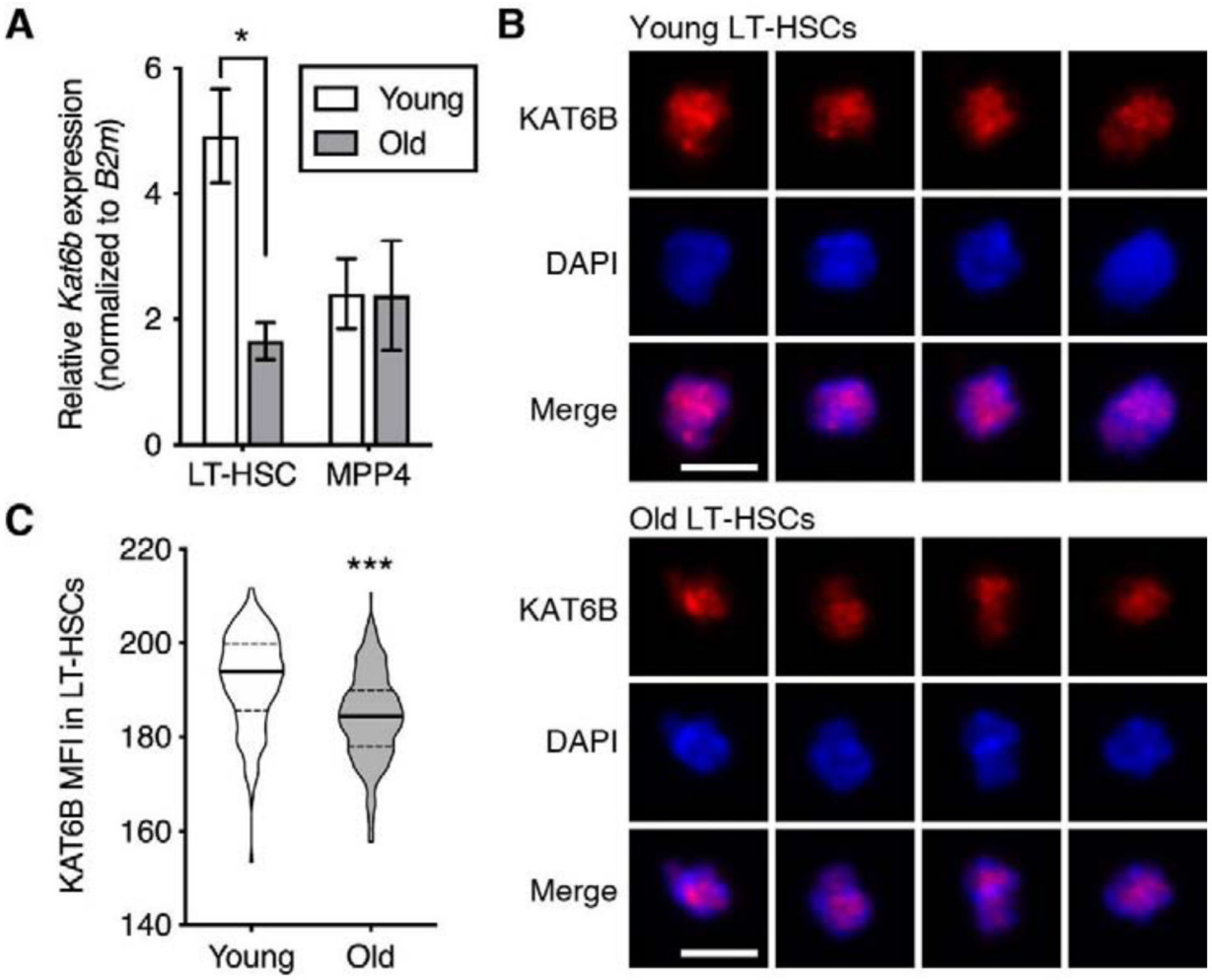

Figure 2. KAT6B is decreased in old LT-HSCs.

(A) Relative expression of *Kat6b* in LT-HSCs and MPP4 cells isolated from young (2–4 month) and old (20–23 month) mice. Bars represent mean ± SEM of $n \geq 3$ biological replicates. *$P < 0.05$ by unpaired *t* test. (B) Representative immunofluorescence images of KAT6B and DAPI in LT-HSCs isolated from young and old mice. Scale bar equals 5 um. (C) Violin plots of mean fluorescence intensity (MFI) of KAT6B in LT-HSCs isolated from young and old mice. Solid lines indicate median and dotted lines indicate quartiles. Data points include $n = 17–64$ individual cells sampled from $n = 4$ biological replicate animals. ***$P < 0.001$ by unpaired *t* test.

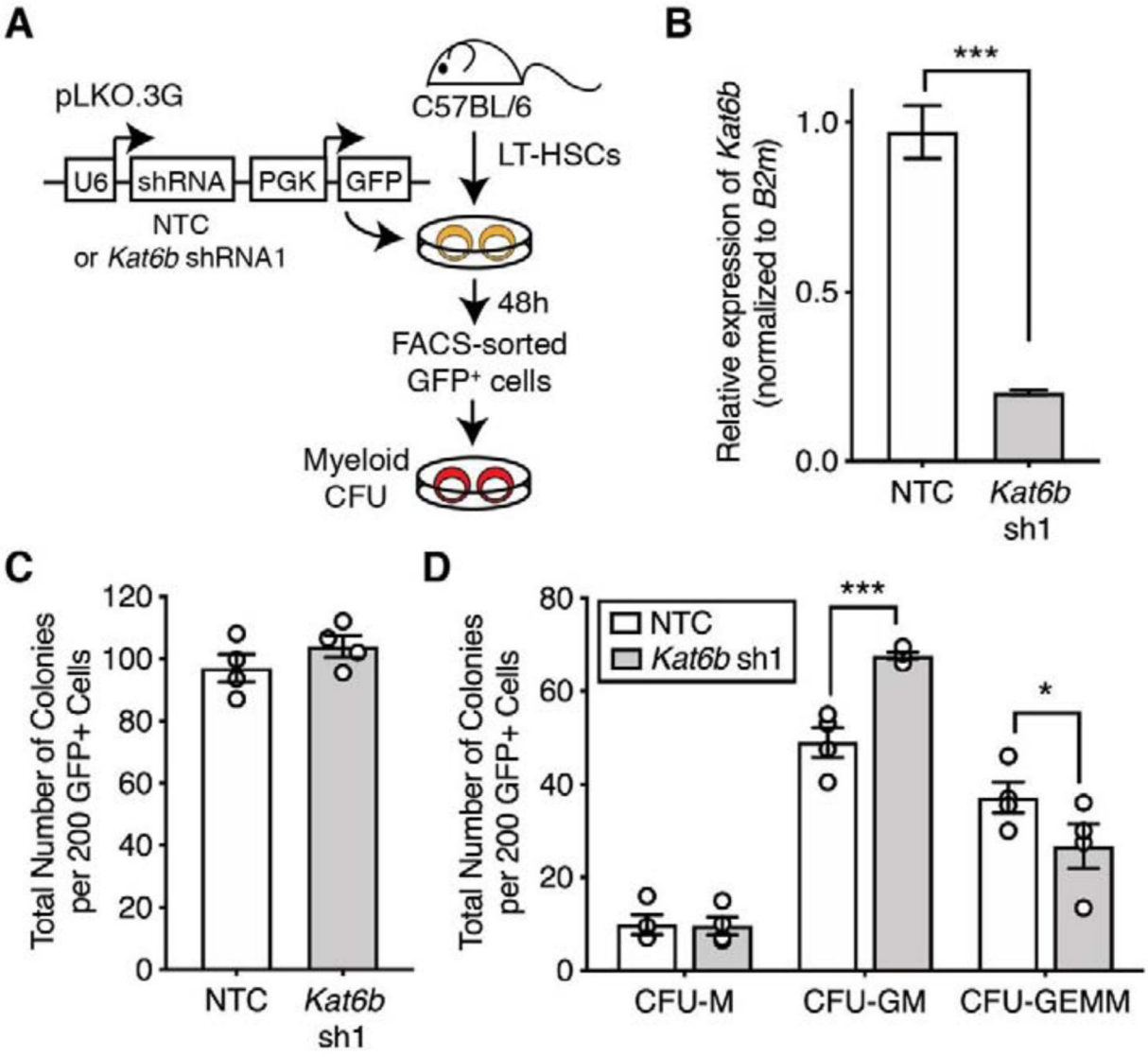

Figure 3. *Kat6b* knockdown results in loss of erythropoietic activity from phenotypic LT-HSCs *in vitro*.

(A) Schematic of experimental design to knockdown *Kat6b* in LT-HSCs and assess differentiation in the myeloid CFU assay. (B) Relative expression of *Kat6b* in colonies following shRNA-mediated knockdown of *Kat6b* or NTC. Bars represent mean ± SEM of $n \geq 3$ biological replicates performed in independent experiments. ***$P < 0.001$ by unpaired t test. (C) Total number of colonies produced and (D) colony subtype distribution from 200 GFP^+ cells post-transduction of LT-HSCs. CFU-M; macrophage, CFU-GM; granulocyte-macrophage, CFUGEMM; granulocyte-erythrocyte-macrophage-megakaryocyte. Dots denote biological replicates and bars represent mean ± SEM of $n \geq 3$ biological replicates performed in independent experiments. *$P < 0.05$; ***$P < 0.001$ by unpaired t test.

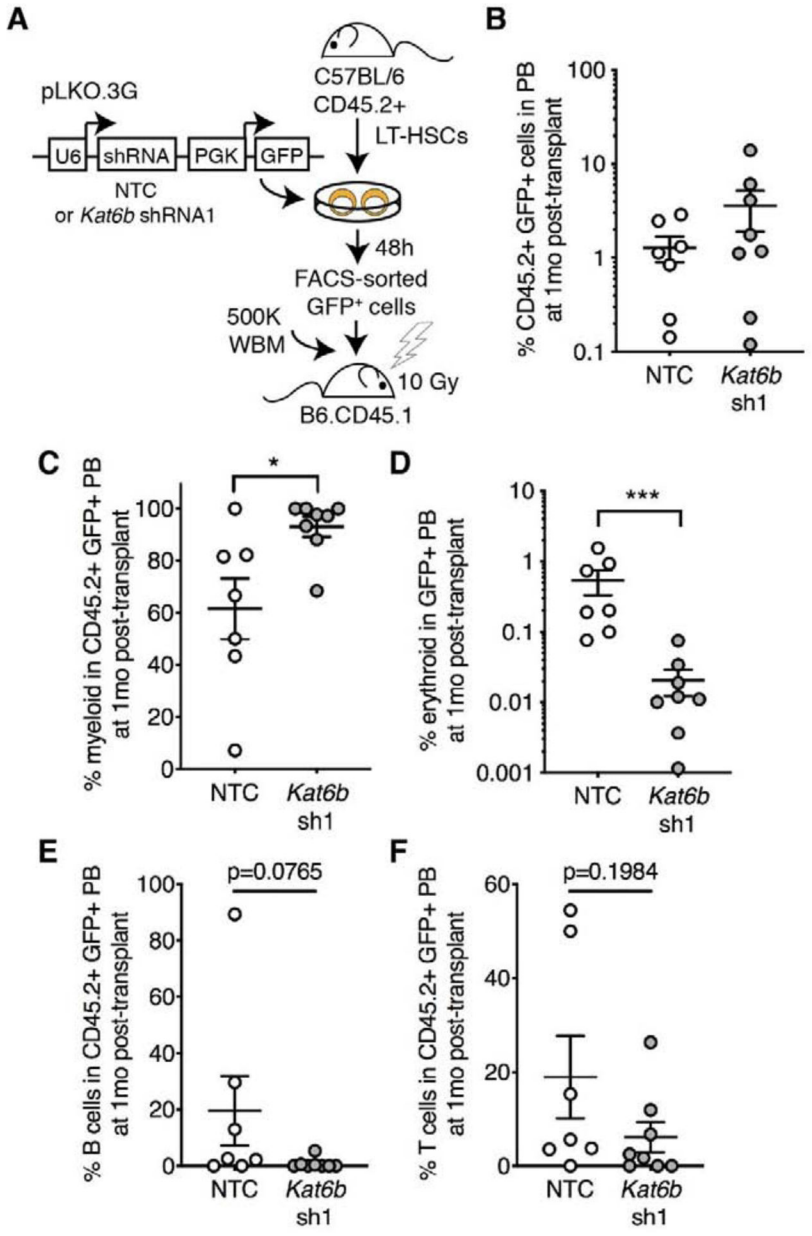

Figure 4. *Kat6b* knockdown alters myeloid and erythroid differentiation of phenotypic LT-HSCs *in vivo*.

(A) Schematic of experimental design to knockdown *Kat6b* in LT-HSCs and assess hematopoietic reconstitution in lethally irradiated recipient mice compared to NTC-transduced LT-HSCs. (B) Frequency of donor-derived cells ($CD45.2^+$ GFP^+) in the PB of recipient mice, (C) myeloid cells ($CD11b^+$) within donor-derived PB cells ($CD45.2^+$ GFP^+), and (D) erythroid cells ($Ter119^+$) within donor-derived PB cells (GFP^+) at 1 month (1mo) post-transplant. (E) Frequency of B cells ($B220^+$) and (F) T cells ($CD3^+$) within donor-derived PB cells at 1mo post-transplant. Each dot represents one recipient mouse. Lines represent mean ± SEM of $n \geq 7$ biological replicates. *$P < 0.05$; ***$P < 0.001$ by Mann-Whitney test.

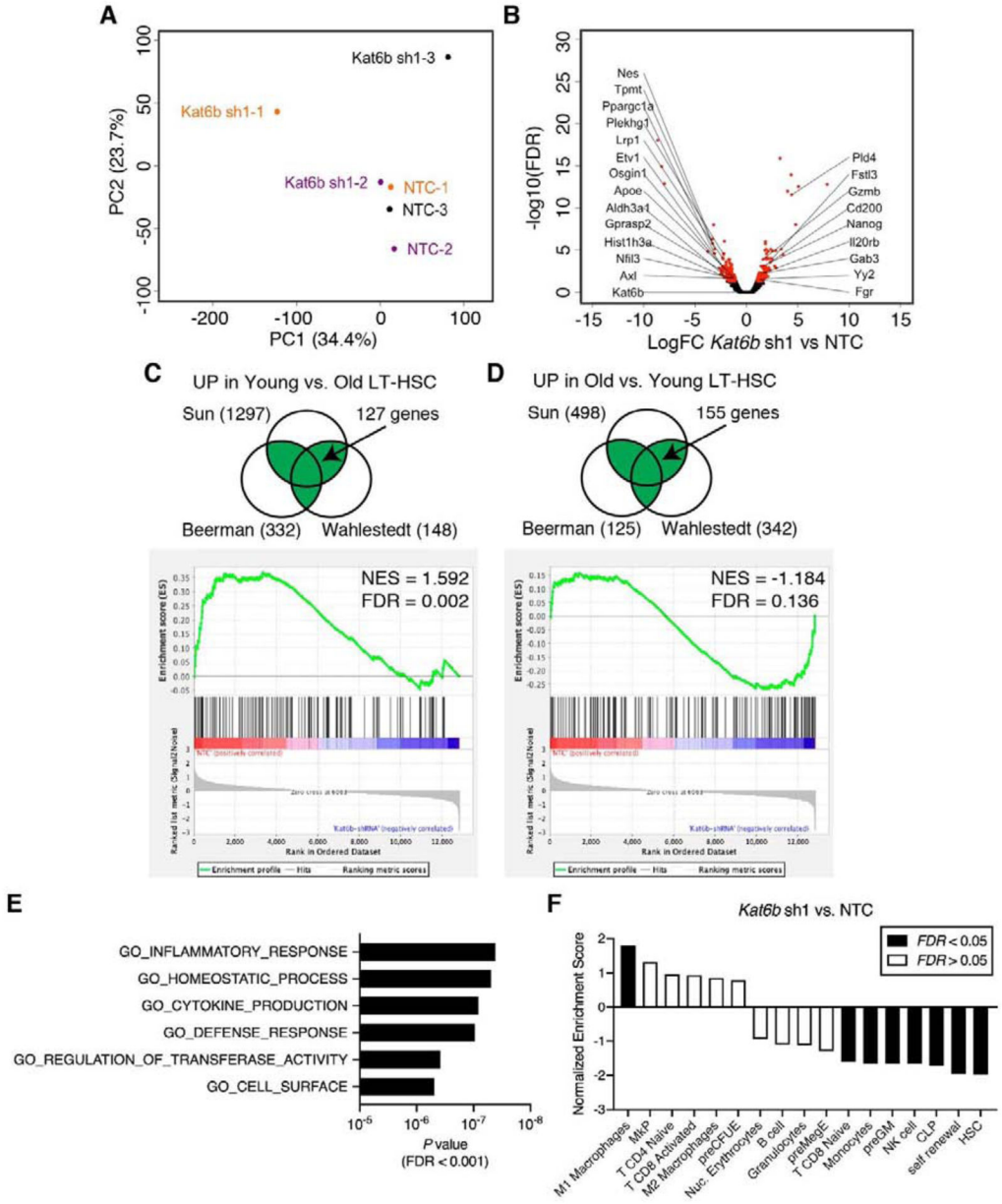

Figure 5. *Kat6b* knockdown alters gene expression programs critical for multilineage differentiation.

(A) PCA plot showing unsupervised clustering of gene expression profiles from *Kat6b* sh1 ($n = 3$) and NTC ($n = 3$). Each color represents a set of biological replicate samples. (B) Volcano plot showing log fold changes of genes against -log10 of *FDR*. Points in red highlight genes with $FDR < 0.05$. (C) Intersection of gene signatures upregulated in young versus old LT-HSCs (top) and GSEA of NTC and *Kat6b* sh1 RNA-seq data using this derived signature (bottom). (D) Intersection of gene signatures upregulated in old versus young LT-HSCs (top) and GSEA of NTC and *Kat6b* sh1 RNA-seq data using this derived signature (bottom). (E) Top GO terms enriched in genes found to be significantly differentially expressed in *Kat6b* sh1 versus NTC (fold change > 2 and $P < 0.05$). (F)

Normalized enrichment score from GSEA analysis of the indicated datasets in *Kat6b* sh1 versus NTC. Black bars indicate $FDR < 0.05$, white bars indicate $FDR > 0.05$.